Transport in Porous Media **23:** 1–30, 1996.

Review Article:

Hydraulic Conductivity of Rock Fractures

ROBERT W. ZIMMERMAN[1,2] and GUDMUNDUR S. BODVARSSON[1]
[1]*Earth Sciences Division, Lawrence Berkeley Laboratory, Berkeley, CA 94720, U.S.A.*
[2]*Earth Resources Engineering Dept., Imperial College, London SW7 2BP, U.K.*

(Received: 15 February 1995; in final form: 7 September 1995)

Abstract. The flow of a single-phase fluid through a rough-walled rock fracture is discussed within the context of fluid mechanics. The derivation of the 'cubic law' is given as the solution to the Navier–Stokes equations for flow between smooth, parallel plates – the only fracture geometry that is amenable to exact treatment. The various geometric and kinematic conditions that are necessary in order for the Navier–Stokes equations to be replaced by the more tractable lubrication or Hele–Shaw equations are studied and quantified. In general, this requires a sufficiently low flow rate, and some restrictions on the spatial rate of change of the aperture profile. Various analytical and numerical results are reviewed pertaining to the problem of relating the effective hydraulic aperture to the statistics of the aperture distribution. These studies all lead to the conclusion that the effective hydraulic aperture is less than the mean aperture, by a factor that depends on the ratio of the mean value of the aperture to its standard deviation. The tortuosity effect caused by regions where the rock walls are in contact with each other is studied using the Hele–Shaw equations, leading to a simple correction factor that depends on the area fraction occupied by the contact regions. Finally, the predicted hydraulic apertures are compared to measured values for eight data sets from the literature for which aperture and conductivity data were available on the same fracture. It is found that reasonably accurate predictions of hydraulic conductivity can be made based solely on the first two moments of the aperture distribution function, and the proportion of contact area.

Key words: fractures, fracture conductivity, Navier–Stokes, Hele–Shaw.

1. Introduction

In many geological formations with low matrix permeability, fluid flow takes place predominantly through fractures. In some cases most of the flow takes place through a single fracture or fault, while in other cases the flow occurs through a network of fractures. In either case, an understanding is needed of how fluid flows through a single rough-walled rock fracture. Fracture-dominated flow is important in many situations of technical or scientific interest, such as in naturally-fractured petroleum reservoirs (van Golf-Racht, 1982; Nelson, 1985), most geothermal reservoirs (Grant *et al.*, 1982), and in many of the sites that have been proposed for underground radioactive waste repositories (Pruess *et al.*, 1990). Various theoretical, numerical and experimental aspects of flow in fractured rock masses are discussed in Bear *et al.* (1993).

In this paper, we address the question of relating the hydraulic conductivity of a single fracture to the geometry and topography of the fracture walls and asperities. We start with the Navier–Stokes equations, which govern the flow of a single-phase fluid, and systematically simplify the equations to reduce them to manageable form, while carefully considering the conditions required in order for the various approximations to be valid. We then discuss and review various analytical and numerical studies that have been done for different types of fracture geometry models. The aim of this discussion is to arrive at an equation that will relate the fracture conductivity to a small number of geometrical parameters, such as the mean aperture, fractional contact area, etc. Finally, we compare the various theoretical models to a few sets of data from the literature in which conductivity and aperture statistics have been measured on the same rock fracture.

2. Basic Equations Governing Fluid Flow

The flow of an incompressible Newtonian viscous fluid is governed by the following form of the Navier–Stokes equations (Batchelor, 1967, pp. 147–150):

$$\frac{\partial \mathbf{u}}{\partial t} + (\mathbf{u} \cdot \nabla)\mathbf{u} = \mathbf{F} - \frac{1}{\rho}\nabla p + \frac{\mu}{\rho}\nabla^2 \mathbf{u}, \tag{1}$$

where ρ is the fluid density, $\mathbf{F}$ is the body force vector (per unit mass), p is pressure, μ is the fluid viscosity, and $\mathbf{u}$ is the velocity vector. The first term on the left represents that portion of the acceleration of a fluid particle that is due to the fact that, at a fixed point in space, the velocity may vary with time. The second term is the advective acceleration term, which accounts for the fact that, even in steady-state flow, a given fluid particle may change its velocity (i.e., be accelerated) by virtue of moving to a position at which there is a different velocity. The sum of these two terms represents the acceleration of a fluid particle computed by 'following the particle' along its trajectory. The terms on the right-hand side represent the applied body force, the applied pressure gradient, and the viscous forces.

Equation (1) represents one vector equation, or three scalar equations, containing four functions: three velocity components and the pressure field. In order to have a closed system of equations, they must be supplemented by the continuity equation, which represents conservation of mass. For an incompressible fluid, conservation of mass is equivalent to conservation of volume, and the equation takes the form

$$\operatorname{div} \mathbf{u} \equiv \nabla \cdot \mathbf{u} = 0. \tag{2}$$

The assumption of incompressibility is acceptable for liquids under typical subsurface conditions. For example, as the compressibility of water is only 4.9×10^{-10}/Pa (Batchelor, 1967, p. 595), a pressure change of 1 MPa (10 bars) will change the density by only 0.05%. The compressibility effect is important for transient problems, since it contributes to the storativity of the rock/fluid system (de Marsily, 1986, pp. 107–108). However, since the relationship between permeability and fracture

geometry is most readily studied using steady-state flow, we will ignore transient effects, and assume that the fluid density is constant. The relevant boundary conditions for the Navier–Stokes equations include the 'no-slip' conditions, which specify that at any boundary between the fluid and a solid, the velocity vector of the fluid must equal that of the solid (Batchelor, 1967, p. 149). This implies that at the fracture walls, not only is the normal component of the velocity equal to zero, but the tangential component vanishes as well.

The most common situation in subsurface flow is for the only appreciable body force to be that due to gravity, in which case $\mathbf{F} = \mathbf{g}$. Taking the z-direction to be vertically upwards, we have $\mathbf{g} = -g\mathbf{e}_z$, where $g = 9.81\,\mathrm{m/s^2} = 9.81\,\mathrm{N/kg}$, and $\mathbf{e}_z$ is a unit vector in the vertical direction. The gravitational term can be removed from the governing equations by defining a reduced pressure (Batchelor, 1967, p. 176; Phillips, 1991, p. 26).

$$P = p + \rho g z, \tag{3}$$

in which case the two terms $\mathbf{F} - (1/\rho)\nabla p$ can be written as

$$\begin{aligned} \mathbf{F} - \frac{1}{\rho}\nabla p &= -g\mathbf{e}_z - \frac{1}{\rho}\nabla p = \frac{-1}{\rho}(\nabla p + \rho g \mathbf{e}_z) \\ &= \frac{-1}{\rho}\nabla(p + \rho g z) = \frac{-1}{\rho}\nabla P. \end{aligned} \tag{4}$$

The governing equations can therefore be written without the gravitational term, in terms of the reduced pressure, P.

Fracture permeability is generally defined under the assumption of steady-state flow under a uniform macroscopic pressure gradient. In the steady-state, the term $\partial\mathbf{u}/\partial t$ drops out, and the equations reduce to

$$\mu\nabla^2\mathbf{u} - \rho(\mathbf{u}\cdot\nabla)\mathbf{u} = \nabla P. \tag{5}$$

The presence of the advective component of the acceleration, $(\mathbf{u}\cdot\nabla)\mathbf{u}$, generally causes the equations to be nonlinear, and consequently very difficult to solve. In certain cases this term is either very small, in which case it can be neglected, or else vanishes altogether. The case of steady flow between parallel plates is one in which the advective terms vanish identically, thus allowing an exact solution to be obtained. If other more realistic geometries are to be considered as models of a rock fracture, approximations must be made to linearize the Navier–Stokes equations, or otherwise reduce them to tractable form.

3. Parallel Plate Model and Cubic Law

The simplest model of flow through a rock fracture is the parallel plate model. This is the only fracture model for which an exact calculation of the hydraulic conductivity is possible; this calculation yields the well-known 'cubic law' (Witherspoon *et al.*,

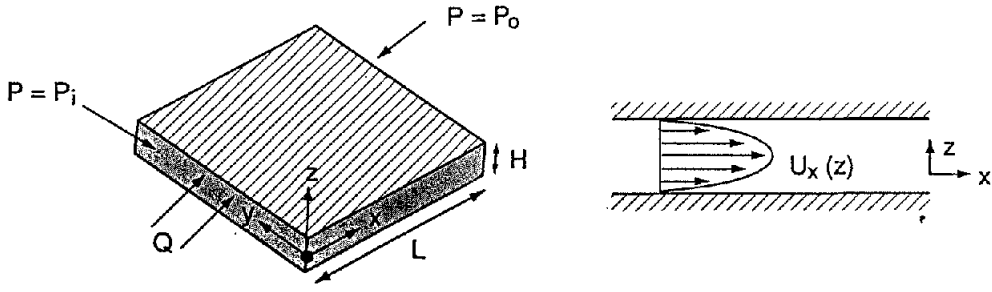

Fig. 1. Parallel-plate fracture of aperture h, with uniform pressures P_i and P_0 imposed on two opposing faces. The resulting parabolic velocity distribution given by Equation (10) is shown on the right.

1980). The derivation of the cubic law begins by assuming that the fracture walls can be represented by two smooth, parallel plates, separated by an aperture h (Figure 1). Now we imagine that there is a uniform pressure gradient within the plane of the fracture. In Figure 1, the magnitude of the pressure gradient is $(P_i - P_0)/L$; it will also be denoted by $|\overline{\nabla P}|$, where the overbar denotes an average over the plane of the fracture. We now set up a Cartesian coordinate system which has its $x_1 \equiv x$ direction parallel to ∇P, its $x_2 \equiv y$ direction perpendicular to x_1 in the plane of the fracture, and its $x_3 \equiv z$ direction (not necessarily vertical) perpendicular to the fracture walls. The top and bottom walls of the fracture correspond to $z = \pm h/2$.

The (reduced) pressure gradient lies entirely in the plane of the fracture, and has no z component. It seems plausible that the velocity will also have no z component, particularly since u_z must not only vanish at the two walls of the fracture, $z = \pm h/2$, but must also have a mean value of zero. Since the geometry of the region between the plates does not vary with x or y, the pressure gradient should also be uniform within the plane of the fracture. Hence, we assume that the velocity vector depends only on z. As all components of the velocity must vanish at $z = \pm h/2$, the velocity vector must necessarily vary with z. The components of the vector $(\mathbf{u} \cdot \nabla)\mathbf{u}$ can be written explicitly as

$$(\mathbf{u} \cdot \nabla)\mathbf{u} = (\mathbf{u} \cdot \nabla)(u_x, u_y, u_z) = [\mathbf{u} \cdot (\nabla u_x), \mathbf{u} \cdot (\nabla u_y), \mathbf{u} \cdot (\nabla u_z)]. \tag{6}$$

The velocity components do not vary with x or y, so any of the three velocity gradients that are not identically zero must be parallel to the z-direction. The velocity vector, on the other hand, is normal to the z-direction. Hence, each of the dot products in Equation (6) is zero. This serves to remove the nonlinear term from Equation (5), leaving

$$\mu \nabla^2 \mathbf{u}(z) = \nabla P. \tag{7}$$

As ∇P lies parallel to the x-axis, it can be written as

$$\nabla P = \left(\frac{\partial P}{\partial x}, \frac{\partial P}{\partial y}, \frac{\partial P}{\partial z} \right) = (|\overline{\nabla P}|, 0, 0). \tag{8}$$

Comparison of Equations (7) and (8) show that the three velocity components must satisfy the following three equations:

$$\nabla^2 u_x(z) = |\overline{\nabla P}|/\mu, \qquad \nabla^2 u_y(z) = 0, \qquad \nabla^2 u_z(z) = 0. \tag{9}$$

The boundary conditions for each velocity component are $u_i = 0$ when $z = \pm h/2$. It is obvious that $u = 0$ will satisfy the governing equations for u_y and u_z, and their associated boundary conditions. To find u_x, we integrate Equation (9a) twice with respect to z, and make use of the boundary conditions, to find the following velocity profile (see Figure 1)

$$u_x(z) = \frac{|\overline{\nabla P}|}{2\mu}[z^2 - (h/2)^2]. \tag{10}$$

This velocity field satisfies the continuity Equation (2), because $u_y = u_z = 0$, and u_x depends only on z, but not on x.

The total volumetric flux through the fracture, for a width w in the y-direction (perpendicular to the pressure gradient), is found by integrating the velocity across the fracture from $z = -h/2$ to $z = +h/2$:

$$\begin{aligned} Q_x &= w \int_{-h/2}^{+h/2} u_x(z)\,\mathrm{d}z \\ &= w \int_{-h/2}^{+h/2} \frac{|\overline{\nabla P}|}{2\mu}[z^2 - (h/2)^2]\,\mathrm{d}z = \frac{-|\overline{\nabla P}| w h^3}{12\mu}. \end{aligned} \tag{11}$$

The average velocity is found by dividing the flux by the cross-sectional area, wh:

$$\overline{u}_x = \frac{Q_x}{wh} = \frac{-|\overline{\nabla P}| h^2}{12\mu}. \tag{12}$$

Now recall Darcy's law for flow through porous media, which in one dimension can be written as (de Marsily, 1986, p. 56)

$$Q = -kA|\overline{\nabla P}|/\mu. \tag{13}$$

The cross-sectional area A is equal to wh, so comparison of Equations (11) and (13) shows that the permeability of the fracture can be identified as $k = h^2/12$. The product of the permeability and area, which is sometimes known as the transmissivity, is equal to

$$T \equiv kA = wh^3/12, \tag{14}$$

Although the transmissivity calculated for the parallel plate model is known as the cubic law, the dependence of T on h^3 is actually a consequence of the fact that the equations must be dimensionally consistent. Since Q_x has units of [m^3/s], the pressure drop has units of [Pa], the length L has units of [m], and μ has units of

[Pa·s], T must have units of [m^4]. As the total flux must scale linearly with the depth w perpendicular to the direction of flow, T must be proportional to the cube of the aperture. Hence, the transmissivity must be of the form $T = Cwh^3$, where C is a dimensionless parameter. It may therefore be said that the main prediction of the parallel plate model is that $C = 1/12$.

4. Deviations from the Cubic Law

The cubic law was derived under the assumption that the fracture consisted of the region bounded by two smooth, parallel plates. Real rock fractures, however, have rough walls and variable apertures. Furthermore, there are usually regions where the two opposing faces of the fracture wall are in contact with each other. Since transmissivity is proportional to h^3, fluid flowing in a variable-aperture fracture under saturated conditions will tend to follow paths of least resistance, which is to say paths of largest aperture, and thereby depart from the rectilinear streamlines of the parallel plate model. In order to use the cubic law to predict the transmissivity of a real rock fracture, one could assume that Equation (14) still holds if the aperture h is replaced by the mean aperture $\langle h \rangle$. This is sometimes taken to be an alternate definition of the cubic law, i.e., (Brown, 1987)

$$T = w\langle h \rangle^3/12. \tag{15}$$

Although Equation (15) is a first approximation to the actual transmissivity of a rough or obstructed fracture, the effects of roughness and obstructions are not properly accounted for by merely replacing h with $\langle h \rangle$, as will be shown below. This suggests that we *define* the so-called hydraulic aperture h_H in terms of the actual transmissivity T, i.e.,

$$T = wh_H^3/12. \tag{16}$$

The problem of relating the transmissivity of a fracture to its geometry can therefore be thought of in terms of finding an expression for the hydraulic aperture h_H. This requires solution of the Navier–Stokes equations in fracture geometries that include varying aperture and obstructed regions.

Another possible cause of deviations from the cubic law is turbulence. The velocity profile given by Equation (10) is an exact solution to the Navier–Stokes equation; however, it is not the *unique* solution to the problem of flow between two smooth parallel plates. In general, there is no uniqueness theorem for the full Navier–Stokes equations, as there is, say, for the equations of linear elasticity. In fact, at sufficiently high velocities, the laminar velocity profile given by Equation (10), although still a solution to the governing equations, will become unstable, giving way to turbulent flow (e.g., Sherman, 1990, Chapter 13). This transition will typically occur when the Reynolds number, which we define as

$$\mathrm{Re} \equiv \rho \overline{u}_x h/\mu, \tag{17}$$

exceeds about 1150 (de Marsily, 1986, p. 66). The Reynolds number is a dimensionless measure of the relative strengths of inertial forces to viscous forces. At low Reynolds numbers, viscous forces are strong enough to damp out any perturbations from the uni-directional, laminar flow field, whereas at sufficiently high velocities small perturbations to the laminar flow field will tend to grow in an unstable manner. Combining Equations (12) and (17) yields the following criterion for the velocity profile (10) to be *stable*:

$$|\overline{\nabla P}| < 13800\mu^2/\rho h^4. \tag{18}$$

This expression shows that high viscosity, low density, and small apertures all tend to stabilize the flow field.

The stability condition given by Equation (18) is satisfied in most subsurface flow situations. For example, consider water with a viscosity of 10^{-3} Pa · s and a density of 10^3 kg/m^3. For fracture apertures as large as 10^{-3} m, laminar flow will be stable for pressure gradients as high as about 1.4×10^7 Pa/m. If the fluid is air, with a viscosity of about 2×10^{-5} Pa · s and a density of about 1.2 kg/m^3 (Batchelor, 1967, p. 175), flow through a 1 mm wide fracture will be stable for pressure gradients up to about 4.6×10^6 Pa/m, or about 46 bars/m. Hence, it seems that genuine turbulent instability will rarely occur during flow through rock fractures. Exceptions include situations of forced fluid flow, such as hydraulic fracturing (Jung, 1989), where large pressure gradients may be developed. For a rough-walled fracture, however, inertial effects due to tortuous flowpaths will lead to deviations from the cubic law long before (i.e., at lower flowrates) genuine turbulence occurs, as will be discussed below.

5. Reynolds Lubrication Approximation

At low flowrates, the two main causes of deviations from the cubic law are roughness of the fracture walls, and asperity contact between the opposing fracture faces. Although asperity contact can be thought of as an extreme case of aperture variation, it is convenient to analyze these two effects separately. First consider the case where the aperture varies from point to point, but is always greater than zero, i.e., no asperity contact. Under certain geometric and kinematic conditions, the Navier–Stokes equations can be reduced to the simpler Reynolds 'lubrication' equation. One necessary condition is that viscous forces dominate the inertial forces (Batchelor, 1967, p. 222). To quantify this criterion, we employ the following order-of-magnitude analysis. Let U be a characteristic magnitude of the velocity, which could be taken to be the average velocity, as given by Equation (12). The velocity varies from 0 at the upper and lower walls to some maximum value of order U at the midplane of the fracture, and this variation occurs over a distance h. Hence, the order of magnitude of the viscous terms in Equation (5) can be estimated to be

$$\text{mag}[\mu\nabla^2\mathbf{u}] \approx \mu U/h^2, \tag{19}$$

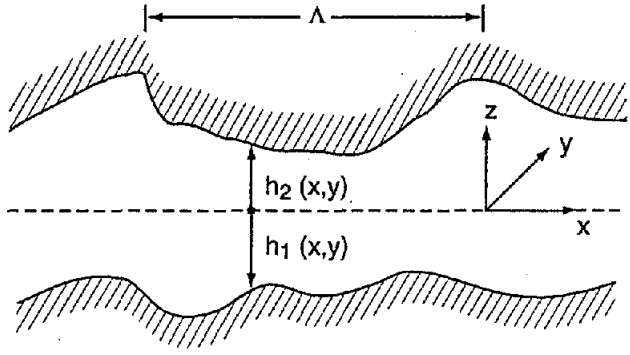

Fig. 2. Side view of a cross-section of a rough-walled rock fracture containing no contact areas. The two half-apertures are h_1 and h_2, both defined as positive. The characteristic length over which the aperture varies appreciably is denoted by Λ.

where h^2 appears due to the fact that there are two derivatives taken with respect to z in the expression $\nabla^2\mathbf{u}$. To estimate the magnitude of the inertial forces, we first define a characteristic length Λ in the x-direction, which may be the wavelength of the aperture variations, or the distance between asperity obstacles, etc. (Figure 2). The velocity gradient is then on the order of U/Λ, and the inertial terms have magnitude

$$\text{mag}[\rho(\mathbf{u}\cdot\nabla)\mathbf{u}] \approx \rho U^2/\Lambda. \tag{20}$$

For the inertia terms to be smaller than the viscous terms, we must have (Schlichting, 1968, p. 109)

$$\rho U^2/\Lambda \ll \mu U/h^2, \quad \text{or} \quad \text{Re}^* \equiv \rho U h^2/\mu\Lambda \ll 1, \tag{21}$$

where the reduced Reynolds number Re^* is defined to be the product of the traditional Reynolds number, $\rho U h/\mu$, and the geometrical parameter h/Λ.

If condition (21) is satisfied, then the advective inertia term $(\mathbf{u}\cdot\nabla)\mathbf{u}$ is negligible compared to the other two terms in Equation (5), and we can replace the nonlinear Navier–Stokes equations (1) with the mathematically linear Stokes 'creeping flow' equations:

$$\mu\nabla^2\mathbf{u} = \nabla P, \tag{22}$$

which can be written in component form as

$$\frac{\partial^2 u_x}{\partial x^2} + \frac{\partial^2 u_x}{\partial y^2} + \frac{\partial^2 u_x}{\partial z^2} = \frac{1}{\mu}\frac{\partial P}{\partial x}, \tag{23a}$$

$$\frac{\partial^2 u_y}{\partial x^2} + \frac{\partial^2 u_y}{\partial y^2} + \frac{\partial^2 u_y}{\partial z^2} = \frac{1}{\mu}\frac{\partial P}{\partial y}, \tag{23b}$$

$$\frac{\partial^2 u_z}{\partial x^2} + \frac{\partial^2 u_z}{\partial y^2} + \frac{\partial^2 u_z}{\partial z^2} = \frac{1}{\mu}\frac{\partial P}{\partial z}. \tag{23c}$$

These three equations must still be accompanied by the continuity Equation (2). Although the linearity of the Stokes equations allows methods such as Green's functions (Pozrikidis, 1987) and separation of variables (Tsay and Weinbaum, 1991) to be invoked, solutions are still difficult to obtain, and unwieldy to utilize and interpret. Hence, it is desirable to further simplify the equations before attempting to solve them for different fracture geometries.

The validity of the Stokes equations requires that the flow rate be sufficiently small. Further reduction to the simpler Reynolds lubrication equation can be obtained under the additional stipulation that any changes in the aperture occur gradually. The magnitudes of the second derivatives of u_x that appear in Equation (23a) can be estimated as

$$\text{mag}\left[\frac{\partial^2 u_x}{\partial x^2}\right] \approx \text{mag}\left[\frac{\partial^2 u_x}{\partial y^2}\right] \approx \frac{U}{\Lambda^2}, \qquad \text{mag}\left[\frac{\partial^2 u_x}{\partial z^2}\right] \approx \frac{U}{h^2}, \tag{24}$$

where we assume that the characteristic lengths in the x- and y-directions are the same for a macroscopically isotropic fracture. Equation (24) shows that if $(h/\Lambda)^2 \ll 1$, the derivatives with respect to x or y will be negligible compared to those with respect to z. Although a reasonable choice of a characteristic magnitude for u_y is not as obvious, the same order-of-magnitude argument nevertheless shows that $\partial^2 u_y/\partial z^2$ is the dominant term on the left-hand side of Equation (23b).

Estimates of the magnitudes of the terms in Equation (23c) are more difficult to make. As u_z must vanish at the top and bottom walls of the fracture, and as the average value of u_z must vanish over the entire fracture plane, it seems reasonable to assume that u_z will be small at all points (x, y, z). But as long as the fluid always fills the entire fracture, this assumption can never be exactly true, except when the aperture is uniform. Abrupt changes in aperture in the x- or y-direction would require the fluid velocity to have a component in the z-direction. As long as the aperture variations are very gradual, i.e., $h/\Lambda \ll 1$, it seems plausible to assume that u_z is negligible. Equation (23c) then implies that $\partial P/\partial z$ is zero, in which case P is a function only of (x, y).

If the aperture varies gradually, and the flowrate is sufficiently low, the Stokes equations (23a–c) can therefore be replaced by

$$\mu\frac{\partial^2 u_x}{\partial z^2} = \frac{\partial P}{\partial x}, \tag{25a}$$

$$\mu\frac{\partial^2 u_y}{\partial z^2} = \frac{\partial P}{\partial y}. \tag{25b}$$

The right-hand sides of Equation (25) do not depend on z, so the equations can be integrated with respect to z, making use of the no-slip boundary conditions at the top and bottom walls, $z = h_1$ and $z = -h_2$ (see Figure 2), to yield

$$u_x(x,y,z) = \frac{1}{2\mu}\frac{\partial P(x,y)}{\partial x}(z-h_1)(z+h_2), \tag{26a}$$

$$u_y(x,y,z) = \frac{1}{2\mu}\frac{\partial P(x,y)}{\partial y}(z-h_1)(z+h_2). \tag{26b}$$

This is essentially the same parabolic profile as was found for the case of constant aperture, Equation (10), except that the velocity is now parallel to the local pressure gradient, which is not necessarily aligned with the overall pressure gradient. We now integrate these velocity profiles from $z = -h_2$ to $z = h_1$, to find

$$\overline{u}_x = \frac{1}{h}\int_{-h_2}^{h_1} \frac{1}{2\mu}\frac{\partial P}{\partial x}(z-h_1)(z-h_2)\,\mathrm{d}z = \frac{-h^2(x,y)}{12\mu}\frac{\partial P}{\partial x}, \tag{27a}$$

$$\overline{u}_y = \frac{1}{h}\int_{-h_2}^{h_1} \frac{1}{2\mu}\frac{\partial P}{\partial y}(z-h_1)(z-h_2)\,\mathrm{d}z = \frac{-h^2(x,y)}{12\mu}\frac{\partial P}{\partial y}, \tag{27b}$$

where the overbar indicates an average taken over the z coordinate, and $h = h_1 + h_2$ is the total aperture.

Equations (27a,b) satisfy the equations of conservation of momentum, Equation (25), but contain an unknown pressure field, $P(x,y)$. The pressure must be found by appealing to some form of the continuity equation. The continuity equation given by Equation (2), however, applies to the actual local velocities, not to the integrated values. But $\nabla \cdot \mathbf{u} = 0$, so the integral of $\nabla \cdot \mathbf{u}$ with respect to z must also be zero. Interchanging the order of these two operations (which is valid as long as the velocity components vanish at $z = h_1$ and $z = -h_2$, as can be proven by applying Liebnitz' rule), then shows that the divergence of the local flux, $h\overline{\mathbf{u}}$, is also equal to zero. Hence, we can apply Equation (2) to the local fluxes given in Equation (27), yielding $\nabla \cdot [h^3 \nabla P] = 0$, i.e.,

$$\frac{\partial}{\partial x}\left[h^3(x,y)\frac{\partial P}{\partial x}\right] + \frac{\partial}{\partial y}\left[h^3(x,y)\frac{\partial P}{\partial y}\right] = 0, \tag{28}$$

which is the equation first derived for lubrication-type flows by Reynolds (1886). Equation (28) has often been derived for flow in fractures (Walsh, 1981; Brown, 1989) by merely assuming that the cubic law holds *locally* at each point in the fracture, and then invoking the principle of conservation of mass. This type of derivation unfortunately does not shed light on the conditions that are required for the lubrication approximation to be applicable.

Equation (28) is a single, linear partial differential equation that describes the pressure field in the fracture plane. Its solution requires prescription of either the

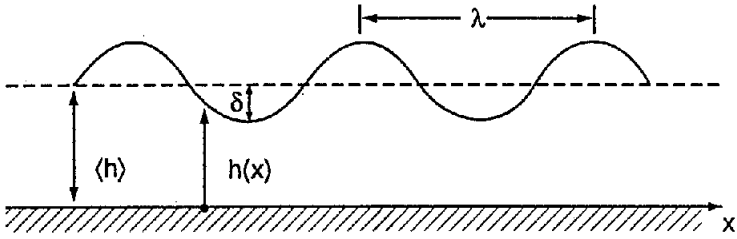

Fig. 3. Side view of a frature channel bounded by one smooth wall and one sinusoidal wall, with the aperture given by Equation (30). The mean aperture is $\langle h \rangle$, the spatial wavelength is λ, and the amplitude of the roughness is δ.

pressures or their normal derivatives (i.e., the fluxes) over the outer boundary of the fracture plane. To find the permeability of a fracture, one would typically solve this equation in a rectangular region defined by $0 < x < L_x, 0 < y < L_y$. The two lateral sides $y = 0$ and $y = L_y$ would be no-flow boundaries, implying that $\overline{u}_y = 0$ at $y = 0$ and $y = L_y$. But Equation (27) shows that $\overline{u}_y$ is proportional to $\partial P/\partial y$, so we see that $\partial P/\partial y = 0$ on the lateral boundaries. The two sides $x = 0$ and $x = L_x$ are constant pressure boundaries, with $P(0, y) = P_i$, and $P(L_x, y) = P_0$. The overall flux is found by integrating $\overline{u}_x$ across the inlet of the fracture:

$$Q_x = \int_0^{L_y} h\overline{u}_x(0, y)\, dy. \tag{29}$$

Finally, the fracture transmissivity is found from $T = Q_x\mu/|\overline{\nabla P}|$. The fracture permeability could be defined as in Equation (14) by dividing by the nominal area of the fracture, $w\langle h \rangle$. The transmissivity is the more useful parameter, however, as its use does not require knowledge of the mean aperture.

6. Range of Validity of the Lubrication Approximation

Reduction of the Navier–Stokes equations to the Reynolds equation requires that the aperture h always be much less than the characteristic spatial wavelength Λ of the aperture variations. It would be useful to have a quantitative measure of how small h/Λ must be in order for this reduction to be permissible. Although rigorous *a priori* error estimates are difficult to derive, some insight into the criterion $h/\Lambda \ll 1$ can be obtained by comparing the Navier–Stokes and Reynolds solutions for a particular geometry that is amenable to analytical treatment. Consider the problem of flow between a smooth wall and a sinusoidally varying wall (Figure 3), with the aperture described by

$$h(x) = \langle h \rangle [1 + \delta \sin(2\pi x/\lambda)]. \tag{30}$$

The aperture does not vary with y, and the macroscopic pressure gradient (and flow) is taken to be in the x-direction.

Hasegawa and Izuchi (1983) performed a perturbation analysis of this problem, using as their small parameters the Reynolds number, $\mathrm{Re} = \rho U \langle h \rangle / \mu$, where U is the mean velocity that would occur if the walls were smooth (i.e., Equation (12)), and the geometrical parameter $\varepsilon = \langle h \rangle / \lambda$. Assuming that the two nonzero velocity components u_x and u_z can be expanded as power series in Re and ε, the standard procedure of regular perturbations then reduces the nonlinear Navier–Stokes equations to a series of linear equations for the coefficients in the power series. Their solution, including the first nontrivial corrections in Re and ε, can be written as

$$k_H^3 = \langle h^{-3} \rangle^{-1} \left[1 - \frac{3\pi^2 (1 - \delta^2) \delta^4}{5(1 + \delta^2/2)} \left(1 + \frac{13}{8085} \mathrm{Re}^2 \right) \varepsilon^2 \right] . \tag{31}$$

The term $\langle h^{-3} \rangle^{-1}$ corresponds to the solution of a one-dimensional version of the lubrication equation (see Equation (38) below). The second term inside the square brackets therefore represents the relative discrepancy between the Navier–Stokes and Reynolds solutions. To see the conditions that must be satisfied by Re and ε in order for this term to be negligible, first let $\mathrm{Re} = 0$. As δ is restricted by definition to lie between 0 and 1, it can be shown that the term that multiplies ε^2 in Equation (31) is always less than 0.662. In order for the error to be less than, say, 10%, we would need $0.662 \langle h \rangle^2 / \lambda^2 < 0.1$, which implies $\lambda > 2.57 \langle h \rangle$. Since the aperture undergoes its maximum variation within a half-wavelength, this condition is equivalent to saying that sizable aperture variations should only occur over distances greater than $\langle h \rangle$. This condition is much less restrictive than the one proposed earlier by Brown (1987), which can, in the present context of a sinusoidal aperture variation, be expressed as $\lambda > 30 \langle h \rangle$. Nevertheless, examination of aperture profiles measured on real rock fractures (Gentier *et al.*, 1989) shows that even this less restrictive condition is not always satisfied.

We now consider the criteria that must be met by Re in order for the correction term in Equation (31) to be small. The term due to nonzero Re is always multiplied by the term due to nonzero $\langle h \rangle / \lambda$. As we have already seen that the Reynolds approximation will break down if λ is not sufficiently small, in order to find restrictions on the allowable values of Re we focus our attention on the worst admissible case, $\lambda = 2.57 \langle h \rangle$, in which case the error is already 10% when $\mathrm{Re} = 0$. If we now assume that at most another 10% error will be tolerated, Equation (31) yields the condition $13\ \mathrm{Re}^2 / 8085 < 1$, which in turn implies $\mathrm{Re} < 25$. However, when $\mathrm{Re} > 1$, it is not permissible to ignore the subsequent terms in the perturbation series, which would be proportional to higher powers of Re, but which were not found by Hasegawa and Izuchi. What can be said with some confidence is that if $\mathrm{Re} < 1$, the error due to a nonzero Reynolds number will be smaller than that due to nonzero $\langle h \rangle / \lambda$. At least for this particular geometry, $\mathrm{Re} < 1$ seems to be a conservative criterion for the validity of the lubrication equation.

When expressed in terms of parameters such as the applied pressure gradient, this criterion takes a form similar to the stability criterion given in Equation (18), except that the maximum Reynolds number is 1 instead of 1150:

$$|\overline{\nabla P}| < 12\mu^2/\rho h^4. \tag{32}$$

The condition for the validity of the Reynolds lubrication equation is therefore stricter, by a factor of about 10^3, than the stability condition for flow in a smooth-walled channel. For a fracture having an aperture of 1 mm, saturated with water of density 1000 kg/m^3 and viscosity 0.001 Pa·s, the pressure gradient must be less than 10^4 Pa/m, or about 0.1 bars/m. This is certainly larger than most naturally-occurring groundwater potential gradients, but will often be exceeded in cases of forced flow (cf., Jung, 1989).

The criterion given by Equation (32) does not merely refer to the validity of the lubrication equation as a mathematical expediency; it also determines whether or not the total flowrate will be a linear function of the pressure gradient. If the Navier–Stokes corrections to the lubrication solution, i.e., the second term in brackets in Equation (31), are negligible, h_H will be independent of the flowrate, and (see Equations (13), (16)) the flowrate will then be directly proportional to $\overline{\nabla P}$. For larger values of Re, Equation (31) shows that h_H will depend on the pressure gradient, in which case Equations (13, 16) show that the flowrate will be a nonlinear function of $\overline{\nabla P}$. Comparison of Equation (32) and Equation (18) shows that the appearance of a nonlinear relationship between Q and $\overline{\nabla P}$ can occur at flowrates that are much less than those required to produce turbulence. This point was made by Bear (1972, p. 178) in the context of flow through three-dimensional porous media. Bear discussed experimental results by Wright (1968) and others that showed nonlinear effects arising at Reynolds numbers as low as 1–10, whereas genuine turbulence did not occur until Re reached about 60–100. Geertsma (1974) pointed out, also in the context of three-dimensional porous media, that in cases of practical importance in petroleum engineering, including converging flow near wellbores, nonlinear departures from Darcy's law occur during laminar, not turbulent, flow. Coulaud *et al.*, (1991) solved the full Navier–Stokes equations numerically for transverse flow past an array of infinitely long, parallel cylinders, and found nonlinearity in the relationship between $\overline{\nabla P}$ and Q to appear at about Re = 2, although the flow was still clearly laminar. Nevertheless, deviations from a Darcy-type linear relationship between $\overline{\nabla P}$ and Q are often attributed, perhaps erroneously, to turbulence (cf., Geertsma, 1974). This issue has been discussed in the specific context of flow through a rock fracture by Holditch and Morse (1976).

7. Numerical Solutions to the Lubrication Equations

Although the lubrication equation is in one sense simpler than either the Navier–Stokes or Stokes equations, because it is a single scalar equation rather than a

vector equation, the presence of the term $h(x, y)$ renders it an equation with variable coefficients. For certain special geometries the equation becomes one-dimensional, and, consequently, easy to solve; these cases are discussed in the next section. For arbitrary isotropic aperture distributions it cannot be solved analytically, but it is amenable to numerical solution procedures (Amadei and Illangasekare, 1992). Several studies have been done in which the equations were solved numerically for various aperture distributions, with the intention of finding some simple relation between the transmissivity and the statistics of the aperture distribution.

Patir and Cheng (1978) used finite differences to solve the lubrication equation for flow between two surfaces whose half-apertures h_1 and h_2 obeyed a Gaussian height distribution with a linearly-decreasing auto-correlation function. They displayed their calculated results as a function of the ratio of the nominal aperture h_0 to the standard deviation of the roughness distribution function, σ_d. The results are shown in Figure 4, in which each data point represents the average of about ten different realizations based on the same values of h_0 and σ_d. For values of h_0/σ_d between 0.5 and 6.0, Patir and Cheng found that the hydraulic aperture could be fit with the function

$$h_H^3 = h_0^3[1 - 0.90\exp(-0.56h_0/\sigma_d)]. \tag{33}$$

The nominal aperture h_0 is therefore a zeroth-order approximation to the hydraulic aperture h_H. The presence of surface roughness decreases the hydraulic aperture below the value h_0. The parameters 0.90 and 0.56 in Equation (33) were chosen so as to fit the data when h_0/σ_d lies between 0.5 and 6.0, and so this equation cannot be thought of as a rigorous first-order correction to the cubic law for small values of the roughness.

An important point to note about the findings of Patir and Cheng concerns the issue of areas at which the two opposing surfaces touch, and the manner in which this affects the definitions of h_0 and σ_d. They defined upper and lower surfaces, the distances of which from the $z = 0$ plane are given by two half-aperture distributions as follows:

$$h_1(x, y) = \frac{h_0}{2} + d_1(x, y), \qquad h_2(x, y) = \frac{h_0}{2} + d_2(x, y), \tag{34}$$

where the functions $d_i(x, y)$ have a mean value of zero. If $h_1 + h_2 > 0$, then the fracture is open at that point, and the aperture is given by $h = h_1 + h_2$. If $h_1 + h_2 \leqslant 0$, i.e., the curves representing the upper and lower surfaces of the fracture overlap each other, then the fracture is assumed to be obstructed at that point, and the aperture is taken to be zero. As pointed out by Brown (1989), the mean aperture $\langle h \rangle$ will equal h_0 if there are no contact regions, but $\langle h \rangle$ will be greater than h_0 if there are contact regions, since the negative values of the function $h = h_1 + h_2$ are not allowed to contribute to the calculation of $\langle h \rangle$. Hence, the parameters h_0 and σ_d used by Patir and Cheng (1978) do not represent the actual mean and standard deviation of the aperture, except for small values of σ_d, when

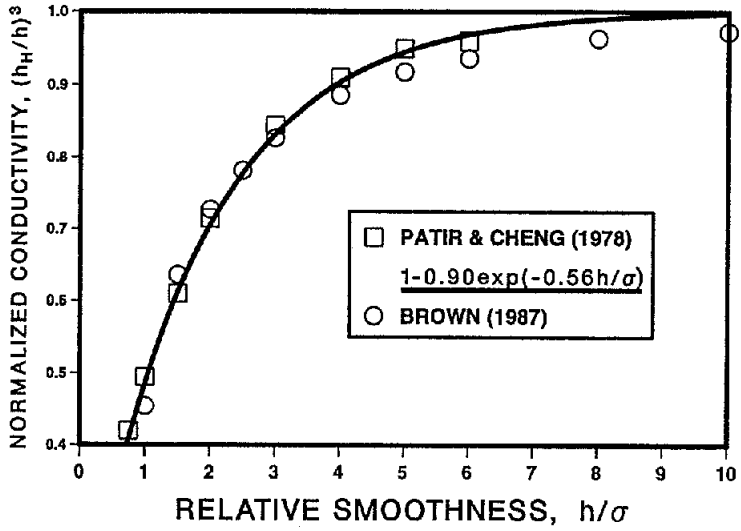

Fig. 4. Results found numerically by Patir and Cheng (1978) and Brown (1987) for the hydraulic aperture as a function of the relative roughness. The slightly different definitions used by h and σ are discussed in the text. Also plotted is Equation (33), which was fitted by Patir and Cheng to their numerical values.

no contact occurs. According to Patir and Cheng, contact regions occurred when $h_0/\sigma_d < 3$, but they did not quantify the amount of contact area that occurred. Therefore, when $h_0/\sigma_d < 3$, the results shown in Equation (33) and Figure 4 represent the combined effects of aperture variation *and* asperity contact.

Brown (1987, 1989) used a finite difference method to solve the Reynolds equation for fractures having randomly-generated, *fractal* roughness profiles. The fractal dimension of the fracture walls varied from 2.0, which represents a smooth wall, to 2.5, which was found by Brown and Scholz (1985) to correspond to a maximum amount of roughness that occurs in real rock fractures. The flow region between fracture walls was formed by generating two surfaces having the same fractal dimension, and then choosing a value for the mean distance between the two planes, h_0. The aperture was then set to zero at any point in the fracture plane where the two fracture walls overlapped. Although Brown presented most of his results in terms of the actual mean aperture $\langle h \rangle$, he followed Patir and Cheng (1978) in using σ_d to quantify the roughness, which is to say, he used the standard deviation of the distance that exists between the two surfaces *before* all negative apertures were set to zero. Hence, it is not possible to replot his data in terms of the actual mean and standard deviation of the *fracture aperture.*

The transmissivities computed by Brown (1987) for a surface having a fractal dimension of 2.5 are plotted on Figure 4, along with the results of Patir and Cheng (1978). Each data point represents the mean of 10 different realizations. Brown found that the fractal dimension had little effect on the computed transmissivities, and that h_H seemed to be mainly a function of $\langle h \rangle$ and σ_d. Brown's mean transmis-

sivities fell very close to the values found by Patir and Cheng (1978), regardless of the fractal dimension of the surface. However, for low values of $\langle h \rangle / \sigma_d$, the unquantified amount of contact area makes it difficult to rigorously compare the two sets of results, since h_0 and $\langle h \rangle$ are not equivalent when there is contact between the two fracture faces.

8. Analytical Treatment of the Lubrication Model

Once the Navier–Stokes equations have been reduced to the Reynolds lubrication equation (28), fluid flow through the fracture is then governed by the same equation that governs, say, heat conduction in an isotropic but inhomogeneous two-dimensional medium. The cube of the local aperture, $h^3(x, y)$, is analogous to the thermal conductivity, k, aside from the multiplicative constant $1/12$ that can be factored out and ignored. A similar equation governs fluid flow in a nearly-horizontal aquifer which has a permeability and/or thickness that varies gradually from point to point (Bear, 1972, p. 215). The problem of finding the effective hydraulic aperture for a fracture that is governed by the Reynolds equation is therefore equivalent to finding the effective conductivity of a heterogeneous two-dimensional conductivity field.

The effective macroscopic conductivity of a heterogeneous medium depends not only on the statistical distribution of the local conductivities, but also on the geometrical and topological manner in which the local conductivity is distributed. If the statistical distribution of conductances is known, but the correlation structure of the conductivity field is either unknown or ignored, upper and lower bounds can be computed for the overall effective conductivity (Beran, 1968, p. 242). These bounds, which are derived using variational principles and certain trial functions for the local pressure field, can be expressed as

$$\left\langle \frac{1}{k} \right\rangle \leqslant k_{\text{eff}} \leqslant \langle k \rangle, \quad \text{or} \quad \langle h^{-3} \rangle^{-1} \leqslant h_H^3 \leqslant \langle h^3 \rangle, \tag{35}$$

where we identify the local conductivity with h^3. The lower bound $\langle 1/k \rangle$ is often called the harmonic mean, whereas the upper bound $\langle k \rangle$ is called the arithmetic mean (de Marsily, 1986, p. 81).

The upper bound can be thought of as corresponding to the hypothetical situation in which all of the conductive elements are arranged in parallel with each other, whereas the lower bound corresponds to a series arrangement of the individual elements (Dagan, 1979). These extreme cases correspond to geometries in which the aperture varies in only one of the two directions, x or y, while the imposed pressure gradient is in the x-direction (see Figure 5). In the case where the aperture varies only in the direction of the applied pressure gradient, the Reynolds Equation (28) reduces to

$$\frac{\mathrm{d}}{\mathrm{d}x} \left(h^3(x) \frac{\mathrm{d}P}{\mathrm{d}x} \right) = 0, \tag{36}$$

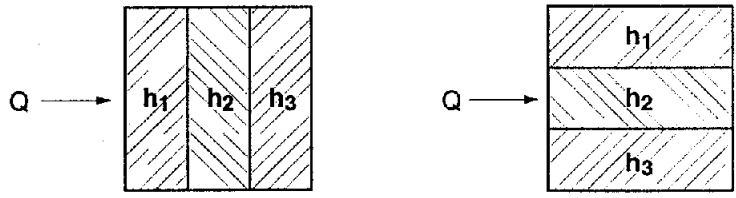

Fig. 5. Fracture in which the aperture varies either only in the direction of flow (top), or only in the direction transverse to the flow (bottom). First case leads to $h_H^3 = \langle h^{-3} \rangle^{-1}$, which is a lower bound on the actual isotropic conductivity. Second case leads to $h_H^3 = \langle h^3 \rangle$, which is an upper bound on the actual isotropic conductivity.

which can be integrated to yield

$$h^3(x)\frac{\mathrm{d}I'}{\mathrm{d}x} = C, \tag{37}$$

where C is a constant of integration. Comparison of Equations (37) and (27a) shows that the constant of integration is equal to $-12\mu(h\overline{u}_x)_0$. A second integration from $x = 0$ to $x = L_x$ yields

$$P_0 - P_i = -12\mu(h\overline{u}_x)_0 \int_0^{L_x} \frac{\mathrm{d}x}{h^3(x)} = -12\mu(h\overline{u}_x)_0 L_x \langle h^{-3} \rangle, \tag{38}$$

which can be rearranged to yield

$$(h\overline{u}_x)_0 = \frac{-|\overline{\nabla P}|}{12\mu}\langle h^{-3} \rangle^{-1}. \tag{39}$$

The total flux is found by integrating $(h\overline{u}_x)_0$ in the y-direction, as in Equation (29), which yields

$$Q_x = \frac{-|\overline{\nabla P}| L_y}{12\mu}\langle h^{-3} \rangle^{-1}. \tag{40}$$

But L_y is equivalent to w, the width of the fracture in the direction normal to the flow, so comparison with Equations (11), (14) shows that this model leads to

$$h_H^3 = \langle h^{-3} \rangle^{-1}, \tag{41}$$

which is identical to the lower bound in Equation (35). An analogous treatment of the case where the aperture varies only in the direction normal to the flow would lead to (Neuzil and Tracy, 1981)

$$h_H^3 = \langle h^3 \rangle, \tag{42}$$

which coincides with the upper bound. These models have been used to estimate the effect of aperture variations on the overall conductivity (Neuzil and Tracy,

1981; Silliman, 1989). However, these types of aperture variations do not lead to macroscopically isotropic behavior. Rather than interpret the bounds given by Equation (35) as representing any specific fracture geometry, we interpret these 'series' and 'parallel' conductances as upper and lower bounds that utilize information about the aperture distribution function, but do not utilize information concerning the spatial correlation of the aperture field.

More restrictive upper and lower bounds on the overall effective conductivity of a heterogeneous medium have been found by Hashin and Shtrikman (1962). For the commonly-assumed case of a log-normal distribution of conductivities, however, these bounds degenerate (Dagan, 1979) into the series and parallel bounds given by Equation (35a). For this case, the 'self-consistent field' approximation has been used (Dagan, 1979), along with a perturbation approach (Dagan, 1993), to approximate the effective conductivity in terms of the mean and standard deviation of the conductivity distribution function. In the case of a statistically isotropic m-dimensional medium, Dagan found

$$k_{\text{eff}} = \langle k \rangle \, \mathrm{e}^{-\sigma_Y^2/2}[1 + (\chi \sigma_Y^2) + (\chi^2 \sigma_Y^4/2) + \cdots], \tag{43}$$

where $Y = \ln(k)$, σ_Y is the standard deviation of $\ln(k)$, and $\chi = (m-2)/2m$. The term in front of the square brackets is equal to the *geometric mean* of the conductivity distribution, k_G, which is defined (in general) by

$$k_G = \mathrm{e}^{\langle \ln(k) \rangle}. \tag{44}$$

The appropriate dimension m for flow in a fracture is 2, in which case $\chi = 0$, leaving

$$k_{\text{eff}} = \langle k \rangle \, \mathrm{e}^{-\sigma_Y^2/2} + \mathrm{O}(\sigma_Y^6). \tag{45}$$

This result can also be expressed as

$$k_{\text{eff}} = \langle k \rangle [1 - (\sigma_Y^2/2) + \cdots]. \tag{46}$$

Although Equation (46) was derived for the specific case of a lognormal conductivity distribution, it can nevertheless be used, *as an approximation*, regardless of the form of the conductivity distribution. For this purpose, it is convenient to express Equations (45), (46) in terms of the standard deviation of k, rather than in terms of the standard deviation of $\ln(k)$. To do this, we first recall that if k is lognormally distributed, then the first two moments of k are related to the first two moments of $Y = \ln(k)$ by (Aitchison and Brown, 1957, p. 11)

$$\langle k \rangle = \mathrm{e}^{\langle Y \rangle + \sigma_Y^2/2}, \qquad \sigma_k^2 = \langle k \rangle^2 [\mathrm{e}^{\sigma_Y^2/2} - 1]. \tag{47}$$

Eliminating σ_Y^2 from Equations (45), (47) yields

$$k_{\text{eff}} \approx \langle k \rangle [1 + \sigma_k^2/\langle k \rangle^2]^{-1/2}, \tag{48}$$

which, to first-order in σ_k^2, can be expressed as

$$k_{\text{eff}} \approx \langle k \rangle [1 - \sigma_k^2 / 2 \langle k \rangle^2 + \cdots]. \tag{49}$$

Equation (49) agrees with the result that can be found from a two-dimensional version of the calculation performed by Landau and Lifshitz (1960, pp. 45–46), who assumed that the conductivity varied smoothly in space about its mean value, $\langle k \rangle$, but did *not* assume that k was lognormally distributed. It therefore is a valid approximation, up to order σ_k^2, for all smoothly-varying two-dimensional conductivity distributions.

We now make use of the identification of k with h^3 to express the above results in terms of the moments of the aperture distribution itself. In general, there is no fixed relationship between $\langle h^3 \rangle$ and $\langle h \rangle$, or between σ_k^2 and σ_h^2. In the case of a lognormal distribution, however, we can make use of the fact that $\ln(k) = \ln(h^3) = 3 \ln(h)$ to find that $\langle \ln(k) \rangle = 3 \langle \ln(h) \rangle$, and $\sigma_{\ln k}^2 = 9 \sigma_{\ln h}^2$ (Aitchison and Brown, 1957, p. 11). Furthermore, if k is lognormally distributed, then so is $h = k^{1/3}$. If we let $z = \ln(h)$, where z has mean value $\langle z \rangle$ and variance σ_z^2, then the statistical moments $\langle h^n \rangle$ are given by (Aitchison and Brown, 1957, p. 8; Gutjahr *et al.*, 1978)

$$\langle h^n \rangle = \mathrm{e}^{n \langle z \rangle + n^2 \sigma_z^2 / 2}. \tag{50}$$

Using these relationships, along with Equation (47), we can rewrite Equations (48), (49) as

$$h_H^3 \approx \langle h^3 \rangle [1 + 9 \sigma_h^2 / \langle h \rangle^2]^{-1/2} \approx \langle h^3 \rangle [1 - 9 \sigma_h^2 / 2 \langle h \rangle^2 + \cdots]. \tag{51}$$

Again using Equation (47), with h in place of k and $z = \ln(h)$ in place of $Y = \ln(k)$, we eventually find that Equation (51) can also be written as

$$h_H^3 \approx \langle h \rangle^3 [1 - 1.5 \sigma_h^2 / \langle h \rangle^2 + \cdots]. \tag{52}$$

Equation (52) indicates that roughness will tend to reduce the hydraulic aperture below the value of the mean aperture. This result is nontrivial, as it can be shown (Silliman, 1989) that the lower bound on h_H given by Equation (35b) can never exceed $\langle h \rangle$, whereas the upper bound can never be less than $\langle h \rangle$. Hence, the bounds alone are not powerful enough to discern whether or not h_H is greater than or less than $\langle h \rangle$. Equation (52) is also in rough agreement with the numerical results of Patir and Cheng (1978) and Brown (1987), particularly when $\langle h \rangle / \sigma_h > 2$, which is the range where, due to lack of substantial contact area, the different definitions of $\langle h \rangle$ and σ_h coincide.

Equation (52) has also been derived by other methods, using specific fracture geometries that did not require lognormal aperture distributions. Elrod (1979) used Fourier transforms to solve the Reynolds equation for a 'fracture' whose aperture had 'sinusoidal ripples in two mutually perpendicular directions', and

arrived at Equation (52) for the isotropic case. Zimmerman *et al.* (1991) considered the case of small regions of unidirectional ripples, as in Equation (30), which were then assembled together so that the direction of striation was randomly distributed. For both sinusoidal and sawtooth profiles, their results agree with Equation (52) up to terms of order $\sigma_h^2/\langle h\rangle^2$. They also examined the effect of higher-frequency sinusoidal components in the aperture profile, using the assumption that the amplitudes of the sinusoidal components scaled with the wavelengths to some positive power, as was found to be the case by Brown and Scholz (1985). (In other words, the small-wavelength roughness will be of small amplitude, so that there will be no sharp dagger-like peaks in the aperture profile.) As long as the results were expressed in terms of $\langle h\rangle$ and σ_h^2, the relationship between h_H, $\langle h\rangle$, and σ_h was essentially unaffected. Hence, it seems that there is much evidence to support Equation (52) as an estimate of the hydraulic aperture in terms of only the mean and standard deviation of the aperture distribution.

If the details of the aperture distribution are known, the geometric mean of h can also be used to estimate h_H, since (Piggott and Elsworth, 1993)

$$h_H^3 = k_{\text{eff}} \approx k_G = e^{\langle \ln k\rangle} = e^{\langle \ln(h^3)\rangle} = e^{3\langle \ln h\rangle} = (e^{\langle \ln h\rangle})^3 = h_G^3. \tag{53}$$

This estimate is accurate to at least $O(\sigma_Y^6)$ for lognormal aperture distributions (Dagan, 1993), but it is not clear that Equation (53) is preferable to Equation (52) in the general case. For example, the numerical simulations of Piggott and Elsworth (1992) indicated that the geometric mean is a very poor predictor of the effective conductivity when the conductivity follows a bimodal distribution, particularly in two dimensions (see also Warren and Price, 1960, Figure 7).

9. Effect of Contact Areas

The areas where the rock faces are in contact with each other can be thought of as regions where the aperture is zero. However, most of the methods used to estimate or bound h_H will break down if the aperture distribution function takes on zero values at any region of the fracture plane that has non-zero measure. For example, the harmonic mean of k, which provides a lower bound to the effective conductivity, will degenerate to zero in these cases, as will the the geometric mean, since a finite probability of having $k = 0$ will cause $\langle \ln(k)\rangle \to -\infty$. These facts suggest using methods such as those discussed above for the regions where the fracture is open, and treating the contact regions by separate methods (cf., Walsh, 1981; Piggott and Elsworth, 1992).

To isolate the effect of contact areas, we consider a fracture for which the aperture is uniform and equal to h_0, except for isolated contact regions where $h = 0$ (Figure 6). Flow through this sort of geometry could, in principle, be analyzed by solving the full Navier–Stokes equations. As this is not practical, we again reduce the governing equations to a more tractable form. Following the procedure by

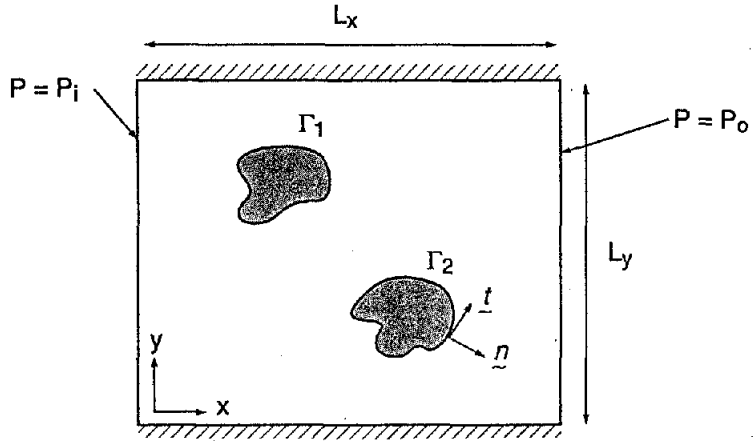

Fig. 6. Schematic diagram of computational problem for the Hele–Shaw model, with impermeable boundaries at $y = 0$ and $y = L_y$, constant pressure boundaries at $x = 0$ and $x = L_x$, and two internal impermeable boundaries that represent the asperity regions.

which the lubrication equation was derived for flow in smoothly-varying channels, we again find the requirements

$$\mathrm{Re}^* \equiv \rho U h^2/\mu\Lambda \ll 1 \quad \text{and} \quad h/\Lambda \ll 1, \tag{54}$$

where now the characteristic lengthscale in the plane of the fracture, Λ, should be identified with, say, the dimensions in the (x, y) plane of the typical contact region (see Figure 6). We again arrive at the lubrication equation (28), except that since $h = 0$ in those regions of the plane where the fracture faces are in contact, the equation has no meaning in those regions. Hence, we can only use this equation in the unobstructed regions, where $h(x, y) = h_0$, where Equation (28) reduces to Laplace's equation:

$$\nabla^2 P(x, y) \equiv \frac{\partial^2 P}{\partial x^2} + \frac{\partial^2 P}{\partial y^2} = 0. \tag{55}$$

This mathematical model of flow between a pair of parallel plates that are obstructed by cylindrical posts is known as the Hele–Shaw model (Bear, 1972, pp. 687–692).

The boundaries Γ_i of the contact regions must be treated as boundaries of the region in the (x, y) plane where this equation is to be solved. Since no fluid can enter the contact region, the component of the velocity vector normal to Γ_i must be zero. Equation (27) shows that the velocity vector is parallel to the pressure gradient, so we see that

$$\frac{\partial P}{\partial n} \equiv (\nabla P) \cdot \mathbf{n} = 0, \tag{56}$$

where $\mathbf{n}$ is the outward unit normal vector to Γ_i, and n is the scalar coordinate in the direction of $\mathbf{n}$. If we consider a rectangular region such as shown in Figure 6,

with uniform pressures on the $x = 0$ and $x = L_x$ boundaries, no flow on the $y = 0$ and $y = L_y$ boundaries, and no flow across the interior boundaries Γ_i, we have a well-posed boundary value problem for Laplace's equation, which will have a unique solution (see Bers *et al.*, 1964, pp. 152–154).

One difficulty that arises with this model is that, in general, the solution will *not* satisfy the no-slip boundary conditions on the internal boundaries Γ_i. In physical terms, the Hele–Shaw model does not account for viscous drag along the *sides* of the posts. The no-slip condition specifies that not only must the normal component of the velocity vanish, but so must the *tangential* component. But the Hele–Shaw solution will generally yield a nonzero tangential component of the velocity along Γ_i, and will consequently be in error in some small region surrounding each asperity. In the original mathematical derivation of the the Hele–Shaw equations, Stokes (1905, p. 278) hypothesized that the thickness of this region would be on the order of h_0. This was verified by Thompson (1968), who used matched asymptotic expansions to solve the creeping flow equations, Equation (23), for flow between two parallel plates that are propped open by a single cylindrical obstacle of radius a, and found that the relative error in the flux perturbation due to a single obstacle was $1.26h_0/a$. Kumar *et al.* (1991) used the Brinkman equation to further analyze the deviations from the Hele–Shaw model caused by finite values of h_0/a. In the Brinkman model, the obstacles are not explicitly included in the geometry of the problem, but their effect on retarding the flow is represented by a distributed body force that is proportional to the velocity. This body force is found by solving the problem of flow past an array of infinitely long, parallel cylinders (Sangani and Yao, 1988). The results of the Brinkman analysis, along with the experimental data collected from various sources by Zimmerman and Kumar (1991), show that as long as $h_0/a < 1$, deviations from the Hele–Shaw conductivity will be less than 10%. As the criterion $h_0/a < 1$ will be met by most rock fractures, the error incurred through the Hele–Shaw approximation will be negligible. For example, Pyrak-Nolte *et al.* (1987) found that typical average apertures of fractures in crystalline rock are on the order of $10^{-4} - 10^{-5}$ m, whereas asperity sizes (in the fracture plane) are on the order of $10^{-1} - 10^{-3}$ m. Gale *et al.* (1990) measured apertures and asperity dimensions on a natural fracture in a granite from Stripa, Sweden, under a normal stress of 8 MPa, and found average values of $h \approx 0.1$ mm, $a \approx 1.0$ mm.

The problem of creeping flow through a smooth-walled fracture of aperture h_0, propped open by an array of circular cylinders of radii $a \gg h_0$, therefore reduces to the problem of finding the effective conductance of a two-dimensional medium of conductance k_0, and which contains a dispersion of non-conductive, circular obstacles. This is a typical problem in effective medium theory, although it is of a different type than that discussed above in relation to the lubrication model, in which the conductivity varied *smoothly* in space. Various methods that have been proposed to solve this type of problem are reviewed by Hashin (1983). Fortunately, the predictions of the different methods do not diverge appreciably until the areal concentration of obstacles approaches about 0.30, which exceeds the amount of

contact area that usually occurs in rock fractures (see Tsang and Witherspoon, 1981; Pyrak-Nolte *et al.*, 1987). Any reasonable two-component effective medium theory can therefore be used for this problem.

Walsh (1981) used the effective medium theory originally proposed by Maxwell (1873, pp. 360–365), who estimated the effective conductivity of a three-dimensional medium containing a dispersion of non-conductive spheres. In the terminology of the present discussion, Maxwell's method consists of calculating the decrease in flow due to a single asperity of known size and planform, averaging this effect over all shapes and orientations of the asperities, and then equating the resulting decrease in flow to that which would be caused by a single *circular* 'obstruction' which has some effective conductivity k_{eff}. Utilizing the solution for flow around a single circular obstruction in an otherwise uniform flow field (Carslaw and Jaeger, 1959, p. 426), Walsh (1981) found that the hydraulic aperture can be expressed as

$$h_H^3 = h_0^3[(1-c)/(1+c)], \tag{57}$$

where c is the areal fraction of the fracture plane that is occupied by the obstructions. Zimmerman *et al.* (1992) used boundary element calculations to verify the accuracy of this result to within about 2% for asperity concentrations up to 0.25. If Equation (52) were applied to a fracture that has aperture h_0 with probability $(1-c)$ and aperture zero with probability c, it would predict $h_H^3 = h_0^3(1 - 1.5c + \cdots)$, which to first order in c is somewhat, although not substantially, different from Equation (57).

The bracketed term in Equation (57) reflects the tortuosity induced into the streamlines by the obstacles, so it would be expected to depend on the planform of the asperity region. Zimmerman *et al.* (1992) extended Walsh's result to the case where the asperities were a randomly-distributed and randomly-oriented collection of ellipses, utilizing the basic solution to two-dimensional flow around an elliptical obstacle that was derived by Obdam and Veling (1987). For ellipses of aspect ratio α, the hydraulic aperture was found to be given by

$$h_H^3 = h_0^3[(1-\beta c)/(1+\beta c)], \quad \text{where} \quad \beta = (1+\alpha)^2/4\alpha. \tag{58}$$

The shape factor in Equation (58) satisfies $\beta \geqslant 1$, and increases monotonically as the ellipse becomes more elongated. Elliptical obstacles therefore obstruct the flow to a greater degree than do circular obstacles. This is consistent with the fact that Walsh's expression for circular obstacles coincides with the Hashin and Shtrikman (1962) theoretical upper bound on k_{eff}/k_0 for a two-component medium with individual conductivities k_0 and 0. Although actual contact areas in fractures are not elliptical in planform, Zimmerman *et al.* (1992) showed that Equation (58) can be applied to a smooth-walled fracture propped open by irregularly-shaped asperities if the actual asperities are 'replaced' by ellipses that have the same perimeter/area ratio.

Another method of accounting for the tortuosity caused by contact areas is to use the effective medium theory of Kirkpatrick (1973), which was originally devised to study electrical conduction in random networks of resistors. This model can be interpreted as corresponding to a checkerboard-like geometry in which each square is randomly assigned an aperture from the actual aperture distribution. In the present context, this corresponds to each square having either aperture h_0 with probability $(1 - c)$, or aperture 0 with probability c. The finite-difference representation of conduction on such a checkerboard geometry would be a square lattice of conductors, in which case Kirkpatrick's theory predicts that

$$h_H^3 = h_0^3(1 - 2c). \tag{59}$$

At low concentrations, Equation (59) agrees with Walsh's result for circular asperities, since each give a tortuosity factor of $(1 - 2c)$, to first order in c. The tortuosity factor predicted by Equation (59) lies below that predicted by the Hashin–Shtrikman upper bound, which is $(1-c)/(1+c)$. It also predicts the existence of a *percolation* limit, which is the value of the contact area (in this case, 0.50) at which flow is completely obstructed. Although it seems reasonable that a sufficiently large amount of contact area will block off all flow paths, contact areas as large as 0.50 have not been reported very often in the literature, so for practical purposes this issue may be irrelevant. Nevertheless, the fact that Equation (59) incorporates the percolation phenomena in some manner is an additional argument for its use in estimating the tortuosity.

10. Comparison of Models to Experimental Data

We now address the question of whether or not the various models and approximations presented and discussed above can be used to quantitatively relate the hydraulic conductance of a fracture to its aperture distribution statistics, bearing in mind that in many cases one might actually be more interested in the inverse problem of determining apertures and contact areas from conductivity data. We will not consider issues related to the measurement of apertures either in the field or in the laboratory, which have been discussed by Gentier *et al.* (1989), Hakami and Barton (1990), and Johns *et al.* (1993), among others. We assume that data are available pertaining to the distribution function of the apertures, and also on the amount (and possibly the shapes) of the contact regions.

Although many measurements of fracture surface roughness have been reported in the literature, as well as many measurements of fracture conductivity, there are very few data sets in which both aperture data and hydraulic conductivity have been measured on the same fracture. Although single fracture surface profiles can be measured in the laboratory, it is problematic to infer from these measurements the aperture formed between two opposing surfaces when they are in contact (cf., Brown *et al.*, 1986; Wang *et al.*, 1988). Many of the measurements upon which certain widely-used roughness-conductivity correlations are based were

TABLE I. Hydraulic transmissivities of fractures in two quartz monzonite granites from Stripa, Sweden. Aperture data and measured conductivities are from Gale *et al.* (1990); the various predictive equations are described in the text.

	S2	S3
$\langle h \rangle$	180	223
σ_h	106	162
c	0.146	0.349
$\langle h^3 \rangle$	7.54	51.8
$\langle h^3 \rangle (1 - 2c)$	5.34	15.6
$\langle h \rangle^3$	5.83	11.1
$\langle h \rangle^3 (1 - 2c)$	4.13	3.35
h_G^3	5.13	5.13
$h_G^3 (1 - 2c)$	3.63	1.55
$\langle h \rangle^3 [1 - 1.5\sigma_h^2 / \langle h \rangle^2]$	2.80	2.31
$\langle h \rangle^3 [1 - 1.5\sigma_h^2 / \langle h \rangle^2](1 - 2c)$	1.98	0.70
h_H^3 (measured)	1.12	0.34

$\langle h \rangle$ and σ_h are given in units of 10^{-6} m; c is dimensionless; other values are in units of 10^{-12} m^3.

actually made on artificially-roughened channels, whose aperture profiles bore little resemblance to those of real fractures (Lomize, 1951; Louis, 1969). We will discuss only those available data sets in which measured fracture conductivities can be directly compared to aperture measurements made on the same fractures. The hydraulic apertures will be predicted using eight different schemes that are suggested by the previously-discussed analyses.

Gale *et al.* (1990) measured the apertures and conductivities of two fractures in a quartz monzonite granite from Stripa, Sweden, using a resin-impregnation technique that allowed aperture measurements to be made on the fracture under the same stress conditions as were used in the flow tests. Data from their two samples, which were taken from the same rock core, are shown in Table I, along with the various predicted values of h_H^3. The values of $\langle h \rangle$ and σ_h were computed directly by Gale *et al.* (1990). We computed $\langle h^3 \rangle$ by assuming that the distribution was lognormal, which is shown by Figures. 3.19 and 3.31 of Gale *et al.* to be a reasonably accurate assumption, in which case Equations (50, 53) can be used to show that $\langle h^3 \rangle = \langle h \rangle^9 / h_G^6$. The values used for h_G are arithmetic means of the h_G values measured on four profiles from each fracture. Since in each case all four profiles were statistically very similar, this method of averaging h_G should yield nearly the same result as would be found by averaging all the individual values of $\ln h$. Table I shows that use of the mean aperture $\langle h \rangle$ in the cubic law, even if corrected for the contact area, will greatly overestimate the actual conductivity. Use

TABLE II. Hydraulic transmissivities of fractures in granite cores from Stripa, Sweden. Aperture data and measured conductivities are from Hakami (1989); the various predictive equations are described in the text.

	B	S2	S3	S4	A1	A2
$\langle h \rangle$	309	464	494	261	83	161
σ_h	193	273	295	98	34	72
$\langle h^3 \rangle$	79.24	243.7	232.0	26.46	0.912	7.209
$\langle h \rangle^3$	29.50	99.90	60.70	17.80	0.572	4.173
h_G^3	18.00	63.96	31.05	14.60	0.453	3.175
$\langle h \rangle^3[1 - 1.5\sigma_h^2/\langle h \rangle^2]$	12.24	48.03	9.397	14.04	0.428	2.921
h_H^3 (measured)	13.14	78.40	14.53	13.31	$< 10^{-4}$	2.406

$\langle h \rangle$ and σ_h are given in units of 10^{-6} m; other values are in units of 10^{-12} m^3.

of $\langle h^3 \rangle$, as was suggested by Neuzil and Tracy (1981), will result in even greater error. The geometric mean h_G is somewhat more accurate, particularly if corrected for the effect of contact area. The most accurate predictions of h_H are those made by using the two-term perturbation estimate, Equation (52), in conjunction with the tortuosity correction, $(1 - 2c)$. More accurate predictions could probably be made by assuming that the contact areas were non-circular, and using the tortuosity factor given by Equation (58). As it is not possible to objectively estimate the equivalent aspect ratio of the contact areas from the available data, we have used Kirkpatrick's 'random lattice' tortuosity factor. Although Brown (1987) did not use precisely the same models as used in Table I to test his numerical solutions of the lubrication equations, it is worth noting that he also found that $\langle h \rangle^3$ was a more accurate predictor of h_H^3 than was $\langle h^3 \rangle$, and that $\langle h \rangle^3(1-c)/(1+c)$ was yet more accurate.

Aperture and hydraulic conductivity measurements were made by Hakami (1989; see also Hakami and Barton, 1990) on epoxy replicas of fractures in five granite cores from Stripa. Sample A was a fine-grained granite, sample B was a leptite, and samples S2, S3, S4 were quartz monzonites. Mean apertures, averaged over areas of about 1 cm^2, were found by injecting a known volume of dyed water into the fracture at various locations, and dividing the volume of the water drop by the observed area it occupied in the plane of the fracture. Although no contact area percentages were reported, the photographs shown of the water drops (Hakami, 1989, p. 46), as well as the aperture histograms at different stress levels (*ibid.*, p. 67), seem to imply that contact area was negligible; this is consistent with the fact that the aperture measurements were made under very low values of normal stress (ibid., p. 66). We will therefore assume $c = 0$ in our calculations. Experimental values, and the various predictions of the hydraulic aperture, are shown in Table II for Hakami's five samples; sample A was measured under two different stresses. We used the values of $\langle h \rangle$ and σ_h corresponding to the best log-normal fit to the

aperture distributions; in most cases these values were well within 10% of the actual values, but for sample S3 this has the effect of ignoring a few anomalously high apertures, which would alter σ_h, but would not be expected to affect h_H. Of the four methods of estimating h_H^3, Equation (52) is in general the most accurate, followed by h_G^3, $\langle h \rangle^3$, and then $\langle h^3 \rangle$. In five of the six cases, both Equation (52) and the geometric mean yield conductivities that are within a factor of two of the measured value. In one case, A1, which was sample A tested under a nonzero normal stress, the measured conductance was extremely low, and was not accurately predicted by any of the methods. No explanation was given for the extremely low permeability measured in this test. Excluding this anomalous case, Equation (52) had an average error (in absolute value) of 21.5%, whereas the geometric mean had an average error of 42.1%. The fact that Equation (52) did not systematically overestimate the conductivity supports our assumption that the contact area correction factor is negligible for these cases.

For both sets of data discussed above, we have found that the expression

$$h_H^3 \approx \langle h \rangle^3 [1 - 1.5\sigma_h^2 / \langle h \rangle^2](1 - 2c) \tag{60}$$

usually provides a good estimate of the fracture conductivity. In fact, it was generally superior to the use of the cube of the geometric mean aperture, even after correction for the tortuosity due to contact area. This latter estimate is equivalent to that suggested by Piggott and Elsworth (1992), with $(1 - 2c)$ used as their tortuosity factor τ. Since there is much theoretical evidence in support of use of the geometric mean in the case of two-dimensional lognormal distributions, whereas the correction given by Equation (52) is only an $O(\sigma^2)$ perturbation approximation, these results call for some explanation. One point to bear in mind is that the actual distributions always deviate somewhat from being lognormal, and in such cases h_G should only be a first-order estimate of h_H. Hence, h_G and Equation (52) are both first approximations to h_H, each in a different sense, for distributions that are slightly perturbed from lognormal. Another point is that some error is introduced when replacing the Navier–Stokes equations with the lubrication equation, Equation (28), due to finite values of $\langle h \rangle / \lambda$, as was discussed previously. Equation (31) implies that these errors tend to *reduce* the effective conductivity below the value predicted by the lubrication model, which may explain the fact that h_G overestimates h_H.

11. Summary

We have discussed the problem of fluid flow through a rock fracture, treating it as a problem in fluid mechanics. First, the 'cubic law' was derived as an exact solution to the Navier–Stokes equations for flow between smooth, parallel plates. For more realistic geometries, the Navier–Stokes equations cannot be solved in closed form, and they must be reduced to simpler equations. The various geometric and kinematic conditions that are necessary in order for the Navier–Stokes equations to be

replaced by the lubrication or Hele–Shaw equations were then studied. A review was given of analytical and numerical studies of the lubrication equation for a rough-walled fracture. Several analytical and numerical studies lead to the conclusion that the hydraulic aperture can be predicted from knowledge of the mean and the standard deviation of the aperture distribution. The tortuosity effect caused by regions where the rock walls are in contact with each other can be accounted for by simple correction factors that depend only on the fractional amount of contact area. Finally, comparison was made between the various predictions of h_H, and the measured values, for eight data sets from two different research groups in which apertures and conductivities were available on the same fracture. The results showed that, in general, reasonably accurate predictions of conductivity could be made by combining either the perturbation result, Equation (52), or the geometric mean, Equation (53), with the tortuosity factor given by Equation (59).

Acknowledgements

This work was carried out under U.S. Department of Energy Contract No. DE-AC03-76SF00098, for the Director, Office of Civilian Radioactive Waste Management, Office of Geologic Disposal, administered by the Nevada Operations Office, U.S. Department of Energy, in cooperation with the United States Geological Survey, Denver. The authors thank Akhil Datta Gupta of Texas A&M, Curt Oldenburg of LBL, Lynn Gelhar of MIT, Ron Linden of the DOE, In-Wook Yeo of Imperial College, and three *TiPM* reviewers, for their constructive comments.

References

Aitchison, J. and Brown, J. A. C.: 1957, *The Lognormal Distribution*, Cambridge University Press, New York.

Amadei, B. and Illangasekare, T.: 1992, Analytical solutions for steady and transient flow in non-homogeneous and anisotropic rock joints, *Int. J. Rock Mech.* **29**, 561–572.

Batchelor, G. K.: 1967, *An Introduction to Fluid Dynamics*, Cambridge University Press, New York.

Bear, J.: 1972, Dynamics of Fluids in Porous Media, Elsevier, New York.

Bear, J., Tsang, C.-F. and deMarsily, G.: 1993, *Flow and Contaminant Transport in Fractured Rock*, Academic Press, San Diego, California.

Beran, M. J.: 1968, *Statistical Continuum Theories*, Interscience, New York.

Bers, L., John, F. and Schechter, M.: 1964, *Partial Differential Equations*, Wiley-Interscience, New York.

Brown, S. R.: 1987, Fluid flow through rock joints: the effect of surface roughness, *J. Geophys. Res.* **92**, 1337–1347.

Brown, S. R.: 1989, Transport of fluid and electric current through a single fracture, *J. Geophys. Res.* **94**, 9429–9438.

Brown, S. R. and Scholz, C. H.: 1985, Broad bandwidth study of the topography of natural rock surfaces, *J. Geophys. Res.* **90**, 12575–12582.

Brown, S. R., Kranz, R. L. and Bonner, B. P.: 1986, Correlation between the surfaces of natural rock joints, *Geophys. Res. Lett.* **13**, 1430–1433.

Carslaw, H. S. and Jaeger, J. C.: 1959, *Conduction of Heat in Solids*, Oxford University Press, Oxford.

Coulaud, O., Morel, P. and Caltagirone, J. P.: 1991, Numerical modeling of nonlinear effects in laminar flow through a porous medium, *J. Fluid Mech.* **190**, 393–407.

Dagan, G.: 1979, Models of groundwater flow in statistically homogeneous porous formations, *Water Resour. Res.* **15**, 47–63.

Dagan, G.: 1993, Higher-order correction of effective permeability of heterogeneous isotropic formations of lognormal conductivity distribution, *Transport in Porous Media* **12**, 279–290.

de Marsily, G.: 1986, *Quantitative Hydrogeology*, Academic Press, San Diego, California.

Elrod, H. G.: 1979, A general theory for laminar lubrication with Reynolds roughness, *J. Lubr. Technol.* **101**, 8–14.

Gale, J., MacLeod, R. and LeMessurier, P.: 1990, Site characterization and validation – Measurement of flowrate, solute velocities and aperture variation in natural fractures as a function of normal and shear stress, stage 3, *Stripa Project Report 90–11*, Swedish Nuclear Fuel and Waste Management Company, Stockholm.

Geertsma, J.: 1974, Estimating the coefficient of inertial resistance in fluid flow through porous media, *Soc. Petrol. Eng. J.* **14**, 445–450.

Gentier, S., Billaux, D. and van Vliet, L.: 1989, Laboratory testing of the voids of a fracture, *Rock Mech. Rock Eng.* **22**, 149–157.

Grant, M. A., Donaldson, I. G. and Bixley, P. F.: 1982, *Geothermal Reservoir Engineering*, Academic Press, New York.

Gutjahr, A. L., Gelhar, L. W., Bakr, A. A. and MacMillan, J. R.: 1978, Stochastic analysis of spatial variability in subsurface flows 2. Evaluation and application, *Water Resour. Res.* **14**, 953–959.

Hakami, E.: 1989, Water flow in single rock joints, Licentiate thesis, Lulea University of Technology, Lulea, Sweden.

Hakami, E. and Barton, N.: 1990, Aperture measurements and flow experiments using transparent replicas of rock joints, in N. Barton and O. Stephansson (eds), *Rock Joints: Proceedings of the International Symposium on Rock Joints*, Balkema, Rotterdam, pp. 383–390.

Hasegawa, E. and Izuchi, H.: 1983, On steady flow through a channel consisting of an uneven wall and a plane wall, Part 1, Case of no relative motion in two walls, *Bull. Jap. Soc. Mech. Eng.* **26**, 514–520.

Hashin, Z.: 1983, Analysis of composite materials – A survey, *J. Appl. Mech.* **50**, 481–505.

Hashin, Z. and Shtrikman, S.: 1962, A variational approach to the theory of the effective magnetic permeability of multiphase materials, *J. Appl. Phys.* **33**, 3125–3131.

Holditch, S. A. and Morse, R. A.: 1976, The effects of non-Darcy flow on the behavior of hydraulically fractured gas wells, *J. Petrol. Technol.* **28**, 1169–1179.

Johns, R. A., Steude, J. S., Castanier, L. M. and Roberts, P. V.: 1993, Nondestructive measurements of fracture aperture in crystalline rock cores using X-ray computed tomography, *J. Geophys. Res.* **98**, 1889–1900.

Jung, R.: 1989, Hydraulic *in situ* investigations of an artificial fracture in the Falkenberg granite, *Int. J. Rock. Mech.* **26**, 301–308.

Kirkpatrick, S.: 1973, Percolation and conduction, *Rev. Mod. Phys.* **45**, 574–588.

Kumar, S., Zimmerman, R. W. and Bodvarsson, G. S.: 1991, Permeability of a fracture with cylindrical asperities, *Fluid Dyn. Res.* **7**, 131–137.

Landau, L. D. and Lifshitz, E. M.: 1960, *Electrodynamics of Continuous Media*, Pergamon Press, New York.

Lomize, G. M.: 1951, *Filtratsiia v Treshehinovatykh Porod (Water Flow in Jointed Rock)*, Gosenergoizdat, Moscow.

Louis, C.: 1969, A study of groundwater flow in jointed rock and its influence on the stability of rock masses, Ph.D. dissertation, Imperial College, London.

Maxwell, J. C.: 1873, *A Treatise on Electricity and Magnetism*, Clarendon Press, Oxford.

Nelson, R. A.: 1985, *Geologic Analysis of Naturally Fractured Reservoirs*, Gulf Publishing, Houston.

Neuzil, C. E. and Tracy, J. V.: 1981, Flow through fractures, *Water Resour. Res.* **17**, 191–199.

Obdam, A. N. M. and Veling, E. J. M.: 1987, Elliptical inhomogeneities in groundwater flow – an analytical description, *J. Hydrol.* **95**, 87–96.

Patir, N. and Cheng, H. S.: 1978, An average flow model for determining effects of three-dimensional roughness on partial hydrodynamic lubrication, *J. Lubr. Technol.* **100**, 12–17.

Phillips, O. M.: 1991, *Flow and Reaction in Permeable Rocks*, Cambridge University Press, New York.

Piggott, A. R. and Elsworth, D.: 1992, Analytical models for flow through obstructed domains, *J. Geophys. Res.* **97**, 2085–2093.

Piggott, A. R. and Elsworth, D.: 1993, Laboratory assessment of the equivalent apertures of a rock fracture, *Geophys. Res. Lett.* **20**, 1387–1390.

Pozrikidis, C.: 1987, Creeping flow in two-dimensional channels, *J. Fluid Mech.* **180**, 495–514.

Pruess, K., Wang, J. S. Y. and Tsang, Y. W.: 1990, On thermohydrologic conditions near high-level nuclear wastes emplaced in partially saturated fractured tuff, 1, Simulation studies with explicit consideration of fracture effects, *Water Resour. Res.* **26**, 1235–1248.

Pyrak-Nolte, L. J., Myer, L. R., Cook, N. G. W. and Witherspoon, P. A.: 1987, Hydraulic and mechanical properties of natural fractures in low permeability rock, in G. Herget and S. Vongpaisal (eds), *Proceedings of the 6th International Congress of Rock Mechanics*, Balkema, Rotterdam, pp. 225–231.

Reynolds, O.: 1886, On the theory of lubrication, *Phil. Trans. Roy. Soc. London* **177**, 157–134.

Sangani, A. S. and Yao, C.: 1988, Transport processes in random arrays of cylinders. II. Viscous flow, *Phys. Fluids* **31**, 2435–2444.

Schlichting, H.: 1968, *Boundary-Layer Theory*, 6th edn., McGraw-Hill, New York.

Sherman, F.: 1990, *Viscous Flow*, McGraw-Hill, New York.

Silliman, S. E.: 1989, An interpretation of the difference between aperture estimates derived from hydraulic and tracer tests in a single fracture, *Water Resour. Res.* **25**, 2275–2283.

Stokes, G. G.: 1905, *Mathematical and Physical Papers*, Cambridge University Press, Cambridge.

Thompson, B. W.: 1968, Secondary flow in a Hele–Shaw cell, *J. Fluid Mech.* **31**, 379–395.

Tsang, Y. W. and Witherspoon, P. A.: 1981, Hydromechanical behavior of a deformable rock fracture subject to normal stress, *J. Geophys. Res.* **86**, 9287–9298.

Tsay, R.-Y. and Weinbaum, S.: 1991, Viscous flow in a channel with periodic cross-bridging fibers: exact solutions and Brinkman approximation, *J. Fluid Mech.* **226**, 125–148.

van Golf-Racht, T. D.: 1982, *Fundamentals of Fractured Reservoir Engineering*, Elsevier, Amsterdam.

Walsh, J. B.: 1981, The effect of pore pressure and confining pressure on fracture permeability, *Int. J. Rock Mech.* **18**, 429–435.

Wang, J. S. Y., Narasimhan, T. N. and Scholz, C. H.: 1988, Aperture correlation of a fractal fracture, *J. Geophys. Res.* **93**, 2216–2224.

Warren, J. E. and Price, H. S.: 1960, Flow in heterogeneous porous media, *Soc. Petrol. Eng. J.* **1**, 153–169.

Witherspoon, P. A., Wang, J. S. Y., Iwai, K. and Gale, J. E.: 1980, Validity of cubic law for fluid flow in a deformable rock fracture, *Water Resour. Res.* **16**, 1016–1024.

Wright, D. E.: 1968, Nonlinear flow through granular media, *Proc. Amer. Soc. Civ. Eng. Hydr. Div.* **94**, 851–872.

Zimmerman, R. W. and Kumar, S.: 1991, A fluid-mechanical model for blood flow in lung alveoli, in J. J. McGrath (ed), *Advances in Biological Heat and Mass Transfer*, ASME Heat Transfer Division Vol. 189, American Society of Mechanical Engineers, New York, pp. 51–56.

Zimmerman, R. W., Chen, D. W. and Cook, N. G. W.: 1992, The effect of contact area on the permeability of fractures, *J. Hydrol.* **139**, 79–96.

Zimmerman, R. W., Kumar, S. and Bodvarsson, G. S.: 1991, Lubrication theory analysis of the permeability of rough-walled fractures, *Int. J. Rock Mech.* **28**, 325–331.